RSC Advances

PAPER

View Article Online
View Journal | View Issue

Cite this: *RSC Adv.*, 2015, **5**, 49662

Hyperbranched fluorene-*alt*-carbazole copolymers with spiro[3.3]heptane-2,6-dispirofluorene as the core and their application in white polymer light-emitting devices†

Yuling Wu,[ab] Jie Li,[ab] Wenqing Liang,[ab] Junli Yang,[ab] Jing Sun,[ab] Hua Wang,[ab] Xuguang Liu,[c] Bingshe Xu*[ab] and Wei Huang[d]

A series of hyperbranched copolymers with fluorene-*alt*-carbazole as the branches and three-dimensional-structured spiro[3.3]heptane-2,6-dispirofluorene (**SDF**) as the core were synthesized by one-pot Suzuki polycondensation. 4,7-Dithienyl-2,1,3-benzothiadiazole (**DBT**) as the orange-light emitting unit was introduced into the backbones to obtain white-light emission. The thermal, photoluminescent (PL), electrochemical and electroluminescent (EL) properties of the copolymers were investigated. The copolymers show great thermal stabilities by the introduction of a carbazole moiety. Besides, the HOMO energy levels of the copolymers were enhanced and the hole injection was improved because of the hole-transporting ability of the carbazole unit. The hyperbranched structures suppress the interchain interactions efficiently, and help to form amorphous films. The copolymers exhibit efficient EL performance as a result of the hyperbranched structure with the incorporation of the carbazole moiety. A quite low turn-on voltage of 5.3 V, a maximal luminance of 7409.5 cd m^{-2} and a luminous efficiency of 4.27 cd A^{-1} were achieved with a CIE coordinate of (0.32, 0.26) for the **PFCzSDF10DBT10** (10 mol% of **SDF** and 0.1 mol% of **DBT**) device. The hyperbranched framework based on fluorene-*alt*-carbazole branches and **SDF** core are attractive candidates for solution-processable white polymer light-emitting device (WPLED) applications.

Received 31st March 2015
Accepted 26th May 2015

DOI: 10.1039/c5ra05713b

www.rsc.org/advances

Introduction

Hyperbranched polymers have recently received considerable interest as light-emitting materials for displays, lighting and other photonic devices.[1–5] Firstly, they are easy to be synthesized by one-pot polymerization with comparable properties to dendritic polymers or other well defined polymers.[6,7] Secondly, hyperbranched polymers with a three-dimensional structure can prevent the aggregation of polymer chains, making the material form amorphous films with good quality, and increase the glass transition temperature (T_g) of the polymers.[4,8,9] Recently, a number of hyperbranched electroluminescent polymers with the three principle colors (red,[10] green[11,12] and blue[13]) have been synthesized, and both emission efficiency and thermal stability were effectively improved with respect to their linear analogies.[14–16] However, white-light-emitting hyperbranched polymers have rarely been reported. Meanwhile, white polymer light-emitting devices (WPLEDs) have been widely recognized owing to their potential applications in large-area full-color and flexible displays combined with a color filter, backlights and solid lighting sources, and their great advantages such as high stability, low price, as well as easy fabrication process.[17–19] A general approach to obtain white-light emission from a single molecule or polymer is to use blue-light emitting and complementary orange-light emitting units.[19–21] In our previous research,[22] white-light emitting from copolymers based on 9,9-dioctylfluorene and 4,7-dithienyl-2,1,3-benzothiadiazole (**DBT**) was realized through the incomplete Förster resonance energy transfer (FRET) from the fluorene segment to **DBT** unit.[23] Polyfluorenes (**PFs**) are shown to be the most promising blue light-emitting materials because of high photoluminescence quantum efficiency, and relatively good chemical and thermal stabilities.[24–26] However, it is hard to

[a]*Key Laboratory of Interface Science and Engineering in Advanced Materials, Taiyuan University of Technology, Taiyuan, 030024, China. E-mail: xubs@tyut.edu.cn*

[b]*Research Center of Advanced Materials Science and Technology, Taiyuan University of Technology, Taiyuan, 030024, China*

[c]*College of Chemistry and Chemical Engineering, Taiyuan University of Technology, Taiyuan, 030024, China*

[d]*Key Laboratory for Organic Electronics & Information Displays (KLOEID), Institute of Advanced Materials, Nanjing University of Posts and Telecommunications (NUPT), Nanjing, 210046, China*

† Electronic supplementary information (ESI) available: ^{1}H NMR and ^{13}C NMR characterization of **DBrCz** and ^{1}H NMR characterization of the copolymers and **PFCzSDF10DBT7**. UV-vis absorption of DBT and PL spectra of **PFCz** in $CHCl_3$ solution (10^{-5} mol L^{-1}), and PL spectra of **DBT** in $CHCl_3$ solution (10^{-5} mol L^{-1}). See DOI: 10.1039/c5ra05713b

balance charge injection owing to the large band gap between the HOMO and LUMO energy levels.[27] Carbazole is a well-known hole-transporting unit as a result of the electron-donating capabilities associated with its nitrogen atom.[13,28] For this reason, to reduce the band gap between the work function of PEDOT:PSS and the HOMO energy levels of the copolymers, and further improve the electroluminescent (EL) performance of the copolymers, carbazole incorporated into the copolymer backbone is a promising strategy.

In this paper, hyperbranched copolymers with 3,6-carbazole-*alt*-2,7-fluorene (**PFCz**) and **DBT** branches and spiro[3.3]heptane-2,6-dispirofluorene (**SDF**) core (10 mol%) were constructed. The three-dimensional-structured **SDF** exhibits great morphological stability and intense fluorescence,[29] and furthermore, its steric hindrance can prevent rotation of the adjacent aryl groups, which reduces close packing and intermolecular interactions between the chromophores in the solid-state.[30] In order to obtain white-light emission, the orange light-emitting unit **DBT** was introduced with different contents from 0.05 mol% to 0.10 mol%. Such a highly branched framework provides a highly efficient white-light electroluminescence.

Experimental section

Materials and characterization

9,9-Dioctylfluorene-2,7-bis(trimethyleneboronate) (**M2**, 99.5%) was purchased from Synwitech. Tetrahydrofuran (THF) and toluene were distilled using standard procedures. Other solvents were used without further purification unless otherwise specified. All reactions were carried out using Schlenk techniques under dry nitrogen atmosphere. ^{1}H NMR and ^{13}C NMR spectra were measured on a Bruker DRX 600 spectrometer, and chemical shifts were reported in ppm using tetramethylsilane as an internal standard. Elemental analysis (EA) was performed with a Vario EL elemental analyzer. Molecular weights and polydispersities of the copolymers were determined using gel permeation chromatography (GPC) on an HP1100 high performance liquid chromatograph (HPLC) system equipped with a 410 differential refractometer, and a refractive index (RI) detector, with polystyrenes as the standard and THF as the eluent at a flow rate of 1.0 mL min^{-1} at 30 °C. The UV-visible absorption spectra were determined on a Hitachi U-3900 spectrophotometer and the PL emission spectra were obtained using a Horiba FluoroMax-4 spectrophotometer at room temperature. Thermogravimetric analysis (TGA) of the copolymers was conducted on a Setaram thermogravimetric analyzer at a heating rate of 10 °C min^{-1} under nitrogen atmosphere. Differential scanning calorimetry (DSC) measurements were performed at both heating and cooling rates of 5 °C min^{-1} under nitrogen atmosphere, using DSC Q100 V9.4 Build 287 apparatus. Atomic force microscopy (AFM) measurements were performed on an SPA-300HV from Digital Instruments Inc. (Santa Barbara, CA) at a tapping mode. Cyclic voltammetry (CV) measurements were performed on an Autolab/PG STAT302 electrochemical workstation with the thin film of the copolymer on the working electrode in a solution of tetrabutylammonium hexafluorophosphate (Bu_4NPF_6, 0.1 M) in acetonitrile (CH_3CN) at a scanning rate of 50 mV s^{-1} at room temperature under nitrogen atmosphere. A Pt plate was used as the counter electrode, and a saturated calomel electrode was used as the reference electrode.

Device fabrication and characterization

Patterned glass substrates coated with indium tin oxide (ITO) (20 Ω square^{-1}) were cleaned by a surfactant scrub, washed successively with deionized water, acetone and isopropanol in an ultrasonic bath, and then dried at 120 °C in a heating chamber for 8 h. A 40 nm-thick poly(3,4-ethylenedioxythiophene): poly(styrenesulfonic acid) (PEDOT:PSS) hole injection layer was spin-coated on top of ITO and baked at 120 °C for 20 min. Thin films (50 nm thick) of the copolymers as the emitting layer were deposited on top of the PEDOT:PSS layer by spin-coating the chlorobenzene solution of the copolymers, followed by thermal annealing at 110 °C for 20 min. Then an electron-transporting layer of 1,3,5-tris(*N*-phenylbenzimidazol-2-yl)benzene (TPBi, 35 nm) and LiF (1 nm) and Al (150 nm) as the cathode were deposited by vacuum evaporation under a base pressure of 5×10^{-4} Pa.[31] The EL spectra and CIE coordinates were measured with a PR-655 spectra colorimeter. The current–voltage–forward luminance curves were measured using a Keithley 2400 source meter and a calibrated silicon photodiode.

Syntheses

Spiro[3.3]heptane-2,6-di-(2′,2″,7′,7″-tetrabromospirofluorene) (**TBrSDF**),[32,33] and 4,7-bis(2-bromo-5-thienyl)-2,1,3-benzothiadiazole (**DBrDBT**)[34–36] were synthesized according to the published literature.

3,6-Dibromo-*N*-(2-ethylhexyl)-carbazole (DBrCz).[37,38] 3,6-Dibromo carbazole (6.50 g, 20 mmol) and adequat tetrabutyl ammonium bromide (TBAB) were added to toluene (100 mL) and potassium hydroxide solution (16 mol L^{-1}, 15 mL). After the solution was stirred for 1 h, 2-ethylhexylbromide (4.26 mL, 25 mmol) was added. The mixture was stirred for 12 h under refluxing, and another 12 h at room temperature. After cooling to room temperature, the mixture was extracted with water and methylene chloride (CH_2Cl_2), dried over anhydrous magnesium sulfate and concentrated. The crude product was purified by column chromatography on silica gel with petroleum ether : CH_2Cl_2 = 5 : 1 as eluent to give **DBrCz** as colorless viscous fluid (6.73 g, 15 mmol) in a 77% yield. ^{1}H NMR (600 MHz, $CDCl_3$) δ (ppm): 7.81 (d, J = 1.8 Hz, 2H, Ph), 7.34 (dd, J_1 = 1.8 Hz, J_2 = 9 Hz, 2H, Ph), 6.93 (d, J = 8.4 Hz, 2H, Ph), 3.65 (t, J = 6.6 Hz, 2H, CH_2), 1.78–1.73 (m, 1H, CH), 1.22–1.04 (m, 8H, CH_2), 0.77 (t, J = 6.6 Hz, 3H, CH_3), 0.73 (t, J = 7.8 Hz, 3H, CH_3); ^{13}C NMR (600 MHz, $CDCl_3$) δ (ppm): 142.58, 131.83, 126.24, 126.03, 114.81, 113.52, 50.46, 42.22, 33.86, 31.67, 27.27, 25.94, 16.95, 13.80. Elemental anal. calcd for $C_{20}H_{23}Br_2N$: C 54.94, H 5.30, N 3.20; found: C 54.90, H 5.33, N 3.21.

General procedure for the synthesis of copolymers PPFCzSDF10DBT5–PFCzSDF10DBT10. To a solution of predetermined amount of the monomers (**DBrCz**, **M2**, **TBrSDF** and **DBrDBT**) in toluene (20 mL) was added an aqueous solution (5 mL) of potassium carbonate (2 M) and a catalytic amount of $Pd(PPh_3)_4$ (2.0 mol%). Aliquat 336 (1 mL) in toluene (5 mL) was added as the phase transfer catalyst. The mixture was vigorously stirred at 90 °C for 3 days. Phenylboronic acid was then added to the reaction mixture, followed by stirring at 90 °C for an additional 12 h. Finally, bromobenzene was added in the same way by heating for 12 h again. When cooled to room temperature, the reaction mixture was washed with 2 M HCl and water. The organic layer was separated, and the solution was added dropwise to excess methanol. The precipitates were collected by filtration, and dried under vacuum. The solid was Soxhlet extracted with acetone for 72 h and then passed through a short chromatographic column using toluene as the eluent to afford the copolymers.

PFCzSDF10DBT5. **DBrCz** (0.153 g, 0.35 mmol), **M2** (0.354 g, 0.55 mmol), **TBrSF** (0.071 g, 0.1 mmol) and **DBrDBT** (0.2 ml, 2×10^{-3} mol L^{-1}). Green powder, yield: 62.9%. ^1H NMR ($CDCl_3$) δ (ppm): 7.88–7.57 (–ArH–), 6.93–6.89 (–ArH–), 3.41–2.93 ($-CH_2-$), 2.21–1.89 ($-C-CH_2-$), 1.18–0.96 ($-CH_2-$), 0.93–0.55 ($-CH_3$).

PFCzSDF10DBT7. **DBrCz** (0.153 g, 0.35 mmol), **M2** (0.354 g, 0.55 mmol), **TBrSF** (0.071 g, 0.1 mmol) and **DBrDBT** (0.28 ml, 2×10^{-3} mol L^{-1}). Light yellow powder, yield: 65.8%. ^1H NMR ($CDCl_3$) δ (ppm): 7.89–7.56 (–ArH–), 6.93–6.81 (–ArH–), 3.42–2.93 ($-CH_2-$), 2.21–1.88 ($-C-CH_2-$), 1.19–0.98 ($-CH_2-$), 0.94–0.60 ($-CH_3$).

PFCzSDF10DBT8. **DBrCz** (0.153 g, 0.35 mmol), **M2** (0.354 g, 0.55 mmol), **TBrSF** (0.071 g, 0.1 mmol) and **DBrDBT** (0.32 ml, 2×10^{-3} mol L^{-1}). Green powder, yield: 59.3%. ^1H NMR ($CDCl_3$) δ (ppm): 8.06–7.42 (–ArH–), 6.94–6.77 (–ArH–), 3.45–3.02 ($-CH_2-$), 2.24–1.87 ($-C-CH_2-$), 1.19–0.95 ($-CH_2-$), 0.94–0.64 ($-CH_3$).

PFCzSDF10DBT10. **DBrCz** (0.153 g, 0.35 mmol), **M2** (0.354 g, 0.55 mmol), **TBrSF** (0.071 g, 0.1 mmol) and **DBrDBT** (0.4 ml, 2×10^{-3} mol L^{-1}). Gray powder, yield: 61.4%. ^1H NMR ($CDCl_3$) δ (ppm): 7.98–7.48 (–ArH–), 6.93–6.78 (–ArH–), 3.39–3.02 ($-CH_2-$), 2.21–1.75 ($-C-CH_2-$), 1.22–0.88 ($-CH_2-$), 0.86–0.45 ($-CH_3$).

Results and discussion

Synthesis and characterization

As shown in Scheme 1, a series of hyperbranched copolymers based on *N*-alkyl and 9-C-alkyl substituted 3,6-carbazole-*co*-2,7-fluorene branches with **SDF** (10 mol%) as the branch point were synthesized by one-pot Suzuki polycondensation in relatively high yields. To obtain white-light emission, the organe-light-emitting unit **DBT** was incorporated into the framework with the feed ratios of 0.05 mol%, 0.07 mol%, 0.08 mol% and 0.10 mol%, and the corresponding copolymers are named as **PFCzSDF10DBT5**, **PFCzSDF10DBT7**, **PFCzSDF10DBT8** and **PFCzSDF10DBT10**, respectively. The synthetic and structural results of **PPFCzSDF10DBT5–PFCzSDF10DBT10** are summarized in Table 1.

The functional groups for Suzuki polycondensation were bromine and trimethyleneboronate. The monomers with bromine group include *N*-(2-ethylhexyl)-carbazole, the branch point spiro[3.3]heptane-2,6-dispirofluorene (**SDF**), and 4,7-dithienyl-2,1,3-benzothiadiazole (**DBT**, ≤0.1 mol%), and the monomers with the trimethyleneboronate group were 9,9-dioctylfluorene. Thus, the fluorene and carbazole monomers distributed alternately in the synthesized polymer branches. Because of the same feed ratios of monomers **DBrCz**, **M2** and **TBrSDF** for copolymers **PPFCzSDF10DBT5–PFCzSDF10DBT10**, their ^1H NMR spectra were quite similar (Fig. S3, ESI,† the proton signals of **DBT** have little effect because of its low content), revealing the similar backbone structures of the copolymers. Taking **PFCzSDF10DBT7** as an example (Fig. S4, ESI†), the actual ratio of monomers **DBrCz**, **M2** and **SDF** was

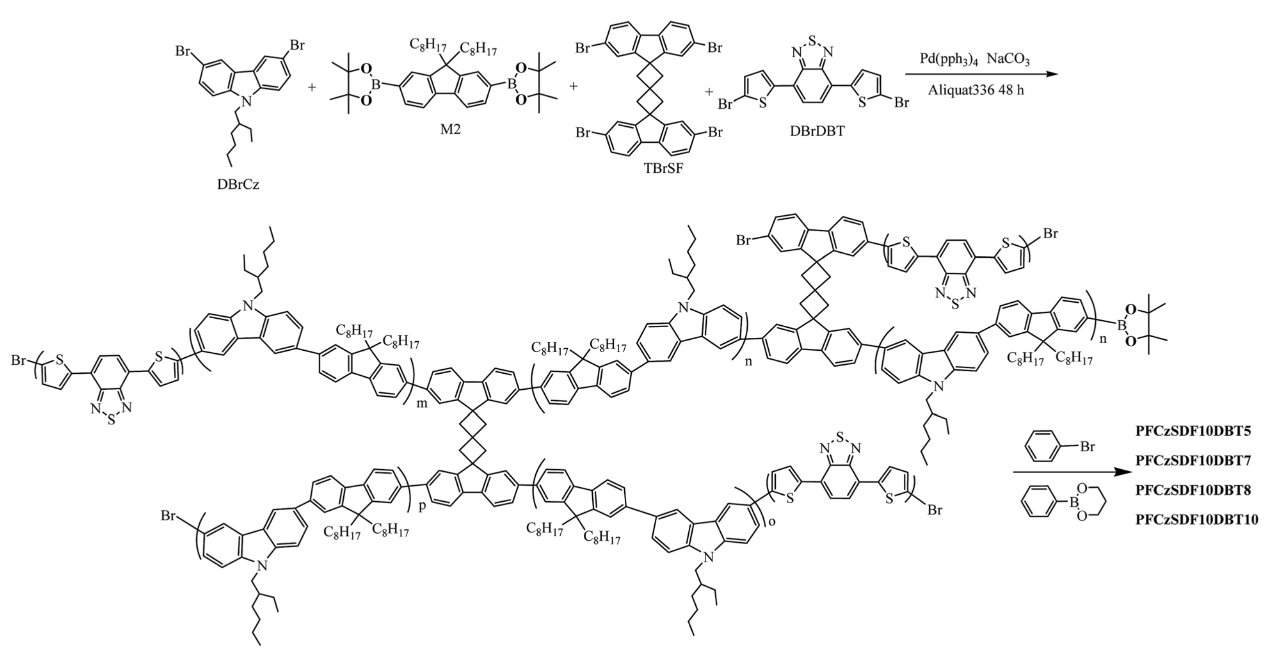

Scheme 1 Synthesis of the hyperbranched copolymers.

Table 1 Polymerization results and characterizations of the copolymers

Copolymers	n_{DBrCz}	n_{M2}	n_{TBrSDF}	n_{DBrDBT}	Yield (%)	GPC M_n	GPC PDI
PFCzSDF10DBT5	0.35	0.55	0.10	5×10^{-4}	62.9	9547	2.29
PFCzSDF10DBT7	0.35	0.55	0.10	7×10^{-4}	65.8	10 535	2.63
PFCzSDF10DBT8	0.35	0.55	0.10	8×10^{-4}	59.3	10 854	2.43
PFCzSDF10DBT10	0.35	0.55	0.10	10×10^{-4}	61.4	10 366	1.60

calculated by comparing the peak integral intensities of the proton signals of α-CH_2 (δ 4.0–4.5), β-CH (δ 1.8–2.2) of *N*-(2-ethylhexyl)-carbazole, β′-CH_2 of 9,9-dioctylfluorene (δ 1.8–2.2), and the spiro[3.3]heptane of **SDF** (δ 3.0–3.5), and the results ($n_{\mathbf{DBrCz}} : n_{\mathbf{M2}} : n_{\mathbf{SDF}}$ 0.35 : 0.54 : 0.1) was quite close to the feed ratio of the monomers (0.35 : 0.55 : 0.1). The number-average molecular weights (M_n) of the copolymers determined by GPC ranged from 9547 to 10 854 with a polydispersity index (PDI) from 1.60 to 2.63. The resulting copolymers are readily soluble in common organic solvents such as $CHCl_3$, THF and toluene.

Thermal properties

The TGA and DSC data of the copolymers are shown in Fig. 1 and Table 2. The onset decomposition temperatures (T_d, measured at a 5% weight loss) range from 400 to 447 °C under nitrogen. The high thermal stability of the copolymers is suggested to benefit from the presence of a large amount of carbazole groups, which are known to exhibit excellent thermal and chemical stabilities.[39] The relatively high glass transition temperatures (T_g, inset of Fig. 1) of the copolymers at around 180 °C are found in the DSC curves, which indicates the good morphological stabilities of the copolymers. The high T_gs of the resulting copolymers could be attributed to their rigid hyperbranched structures and the introduction of carbazole unit to the copolymer backbones.

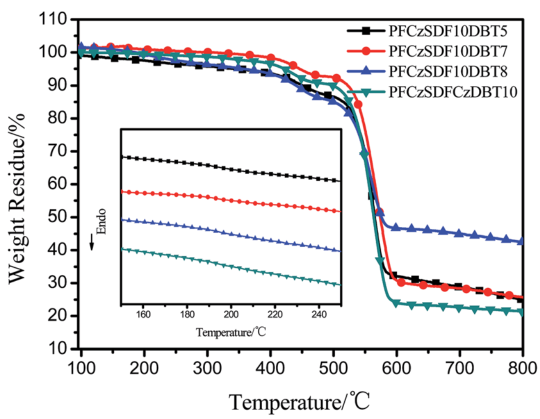

Fig. 1 TGA and DSC (insert) curves of the copolymers in nitrogen atmosphere with a heating rate of 10 °C min^{-1} and 5 °C min^{-1}, respectively.

Photophysical properties

The UV-vis absorption of **DBT** and the PL spectra of fluorene-*alt*-carbazole copolymer (**PFCz**) are shown in Fig. S5a.† The absorption of **DBT** and the emission of **PFCz** show good spectral overlap, indicating the efficient **FRET** from the **PFCz** segment to **DBT** unit can be expected. The normalized UV-vis absorption and PL spectra of the copolymers in dilute solution are shown in Fig. 2a. The absorption bands at around 365 nm are due to the π–π* transitions of poly(fluorene-*alt*-carbazole) backbones,[27] which are blue-shifted about 20 nm compared with the fluorene-based hyperbranched copolymer.[40] This notable hypochromatic shift is attributable to the interruption of the conjugation of the copolymer backbone by the introduction of the 3,6-carbazole linkage. In the PL spectra, the copolymers exhibit emission bands at 416 nm and a slight vibronic shoulder at 436 nm, which can be attributed to the formation of a charge-transfer (CT) state in the poly(fluorene-*alt*-carbazole) branches. The PL spectra showed about 6 nm blue-shift respect to that of the fluorene-based copolymer because of the decreased conjugated length in these fluorene-*alt*-carbazole based copolymers.[40] No distinct absorption or emission peaks of the **DBT** unit can be observed in the spectra because of its comparatively low contents in the copolymers, and the FRET is exclusively intra-chain in dilute solution.[41]

Table 2 Thermal and photophysical properties of the copolymers

Copolymer	T_d (°C)	T_g (°C)	Dilute solution λ_{abs} (nm)	Dilute solution λ_{PL} (nm)	Solid film λ_{abs} (nm)	Solid film λ_{PL} (nm)
PFCzSDF10DBT5	405	186	364	416, 435	370	418, 439
PFCzSDF10DBT7	447	186	362	416, 436	367	417, 437
PFCzSDF10DBT8	400	179	365	416, 436	368	419, 440
PFCzSDF10DBT10	424	178	371	415, 436	372	419, 439, 603

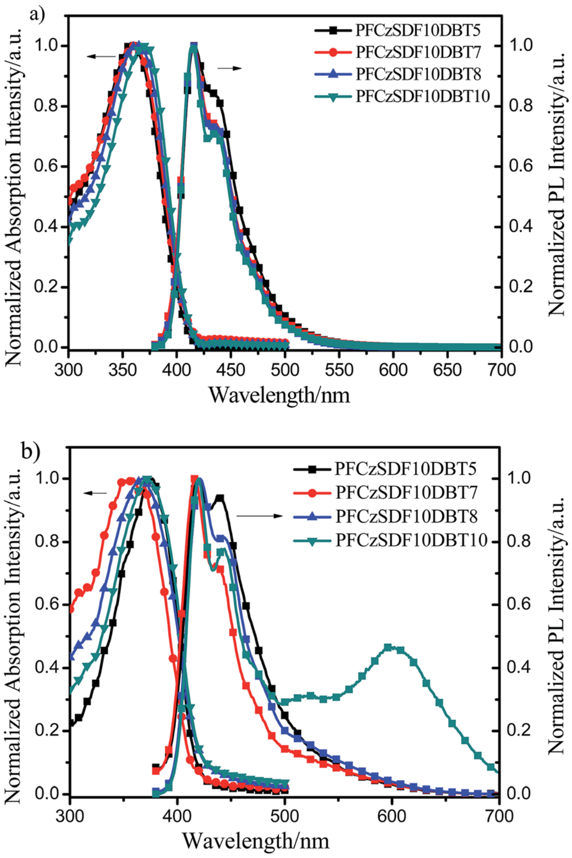

Fig. 2 UV-vis absorption and PL spectra of the copolymers: (a) in $CHCl_3$ solution (10^{-5} M) and (b) in solid film.

In films, the copolymers exhibit UV-vis absorption bands at around 370 nm owning to the π–π* transitions of the poly-(fluorene-*alt*-carbazole) backbones (Fig. 2b and Table 2). In the PL spectra, the maximum emission bands of copolymers are at about 418 nm, along with a shoulder at around 439 nm, showing no obvious bathochromic shift with respect to those in dilute solution. This result indicates that the hyperbranched molecular structure can prevent the aggregation of the copolymer chains efficiently. For **PFCzSDF10DBT10**, the emission band of **DBT** centered at 603 nm can be observed as a result of both intra- and interchain FRET from fluorene-*alt*-carbazole unit to **DBT**, which showed a bathochromic shift of 43 nm compared to that of pure DBT as a result of the conjugation effect of the copolymer system.[23,41,42]

Electrochemical characteristics

The electrochemical behaviors of the resulting copolymers were investigated by cyclic voltammetry (CV), as shown in Fig. 3 and Table 3. The oxidation potentials (E_{ox}) vary slightly from 0.58 to 0.60 V. The HOMO levels of copolymers are calculated according to the empirical formulas $E_{HOMO} = -(E_{ox} + 4.5)$ (eV).[41] The LUMO levels are deduced from the HOMO levels and the optical band gaps (E_g) determined from the onset value of the absorption spectrum in film in the long-wavelength direction ($E_g = 1240/\lambda_{edge}$). The HOMO levels of the hyperbranched copolymers are at about −5.10 eV, which are relatively close to the work function of PEDOT (−5.2 eV) and thus facile hole injection into the emission layer (EML) can be expected.[43] On the other hand, the LUMO levels of copolymers (from −2.08 eV to −2.13 eV) are comparatively distant to the work function of LiF/Al (−2.9 eV), indicating that there is a barrier for electron injection. The results demonstrate that the incorporation of the carbazole moiety into the fluorene backbone could effectively increases the hole-transporting ability of the materials, and at the same time, the potential barrier of electron injection is aggrandized. Thus, an electron transport layer (ETL) will be needed in the following PLED structure.

Film morphology

The morphology of the spin-coated films of the copolymers, which is a key factor for the PLED fabrication, was investigated by atomic force microscopy (AFM) at a tapping mode. Fig. 4 shows the AFM images of **PPFCzSDF10DBT5–PFCzSDF10DBT10** films prepared by spin-coating chlorobenzene solutions of the copolymers (10^{-5} M) on the quartz substrates. Generally, all the films show flat and smooth surface without any pinhole defects. The results imply that the three-dimensional structured **SDF** branch point can help to form homogeneous films with good quality. The uniform amorphous morphology is favorable for PLED fabrication.

Electroluminescent properties

The devices were fabricated with the configuration ITO/PEDOT:PSS (40 nm)/copolymer (50 nm)/TPBi (35 nm)/LiF (1 nm)/Al (150 nm). The relative-energy-level diagram of the devices is shown in Fig. 5. As mentioned above, the incorporation of carbazole unit greatly increases the hole-transporting ability of the materials but leads to a barrier for electron injection into the emission layer. Here 1,3,5-tris(*N*-phenylbenzimidazol-2-yl)benzene (TPBi) is used as the electron-injection layer to facilitate electron transport.[10]

The electroluminescence spectra of the copolymers are shown in Fig. 6, and the device data are summarized in Table 4. The main peaks at 420 nm with a shoulder at 440 nm are analogous to their PL counterparts. The peaks in the long-

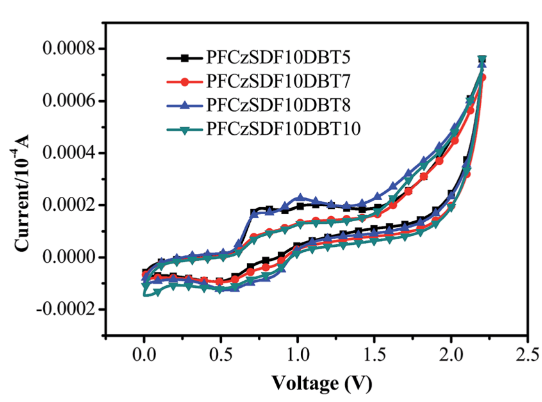

Fig. 3 Cyclic voltammograms of the copolymers.

Table 3 Electrochemical properties of the copolymers

Copolymers	λ_{abs} (onset) (nm)	E_g (eV)	$E_{onset/OX}$ (V)	HOMO (eV)	LUMO (eV)
PFCzSDF10DBT5	416	2.98	0.60	−5.11	−2.13
PFCzSDF10DBT7	412	3.01	0.59	−5.09	−2.08
PFCzSDF10DBT8	418	2.97	0.60	−5.10	−2.13
PFCzSDF10DBT10	419	2.96	0.58	−5.08	−2.12

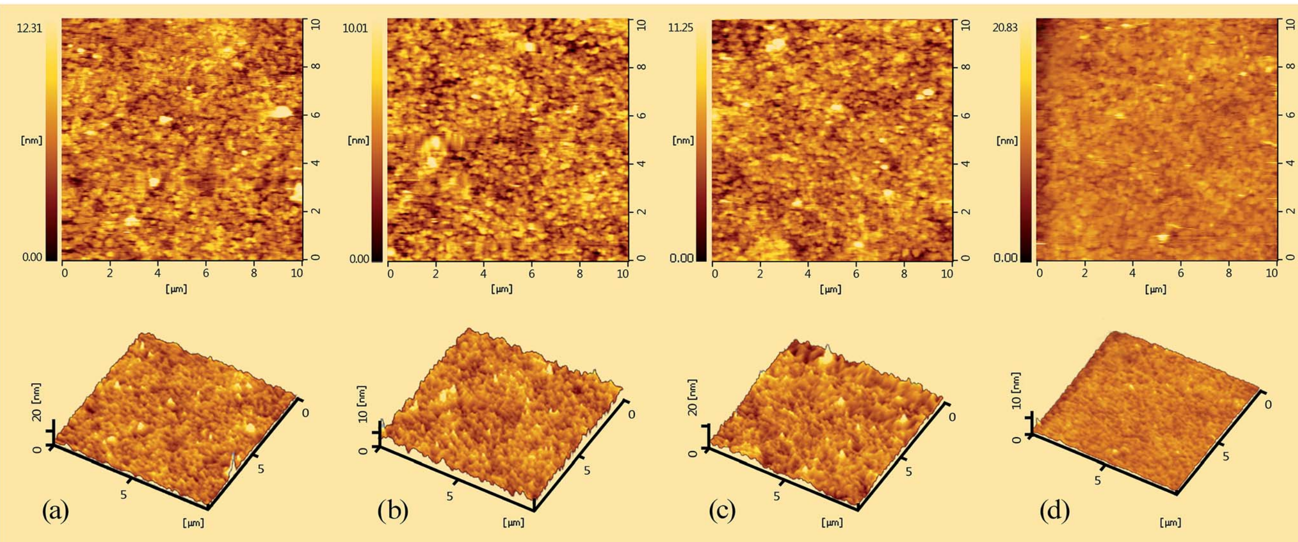

Fig. 4 AFM images (10 × 10 μm) of the copolymer films: (a) PFCzSDF10DBT5, (b) PFCzSDF10DBT7, (c) PFCzSDF10DBT8 and (d) PFCzSDF10DBT10.

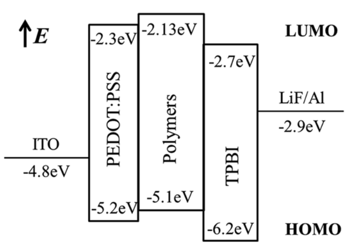

Fig. 5 The energy-level diagram of the devices.

wavelength around 610 nm are gradually enhanced with increasing the contents of the orange-light emission unit **DBT** from **PFCzSDF10DBT5** to **PFCzSDF10DBT10.** White-light emission was obtained with CIE coordinates located near (0.33, 0.33), and the CRI values are around 90 when the contents of **DBT** were 0.08 mol% and 0.10 mol%. **PFCzSDF10DBT8** exhibits cold white light, and **PFCzSDF10DBT10** shows warm white light (Fig. 7).

Taking **PFCzSDF10DBT10** as an example, the mechanism of white light emission was investigated from the EL spectra under voltages varying from 8 V to 13 V (Fig. 8a). It is clearly seen that the spectral stabilities at 420 and 440 nm are extremely well and the broad peaks in the long-wavelength around 610 nm are gradually enhanced with increasing the voltages. The growth rate of the intensity of the peak at 610 nm compared to that at 420 nm accelerates as the voltage increases (Fig. 8b). The results reveal that the intra-, interchain FRET from **PFCz** unit to DBT and the charge trapping of DBT with narrow-band gap happen simultaneously in the electroluminescence process, and the charge trapping is more efficient under higher voltage.[23] So the white-light emission of copolymer **PFCzSDF10DBT10** was

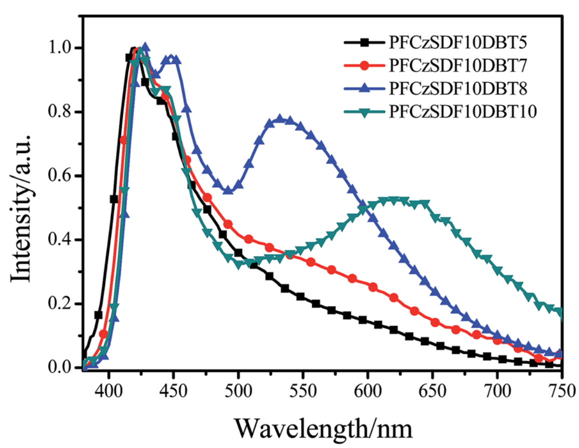

Fig. 6 Electroluminescence spectra of the copolymer PLEDs at a voltage of 13 V.

Table 4 EL performances of the PLEDs

Copolymer	V_{on} [a] (V)	L_{max} [b] (cd m^{-2}) (at the voltage (V))	CE_{max} (cd A^{-1})	LE_{max} (lm W^{-1})	CIE (x,y)
PFCzSDF10DBT5	5.11	7280 (12.6)	4.38	1.64	(0.22,0.20)
PFCzSDF10DBT7	5.24	7188.5 (13.2)	4.02	1.31	(0.25,0.24)
PFCzSDF10DBT8	5.49	7266.4 (13.5)	4.21	1.19	(0.28,0.31)
PFCzSDF10DBT10	5.34	7409.5 (13.5)	4.27	1.45	(0.32,0.26)

[a] Turn-on voltage (at 1 cd m^{-2}). [b] Maximum luminance at applied voltage.

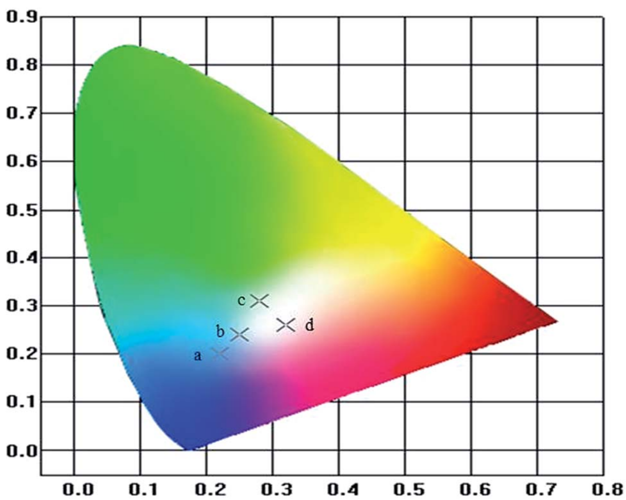

Fig. 7 CIE coordinates of the copolymer PLEDs: (a) **PFCzSDF10DBT5**, (b) **PFCzSDF10DBT7**, (c) **PFCzSDF10DBT8** and (d) **PFCzSDF10DBT10**.

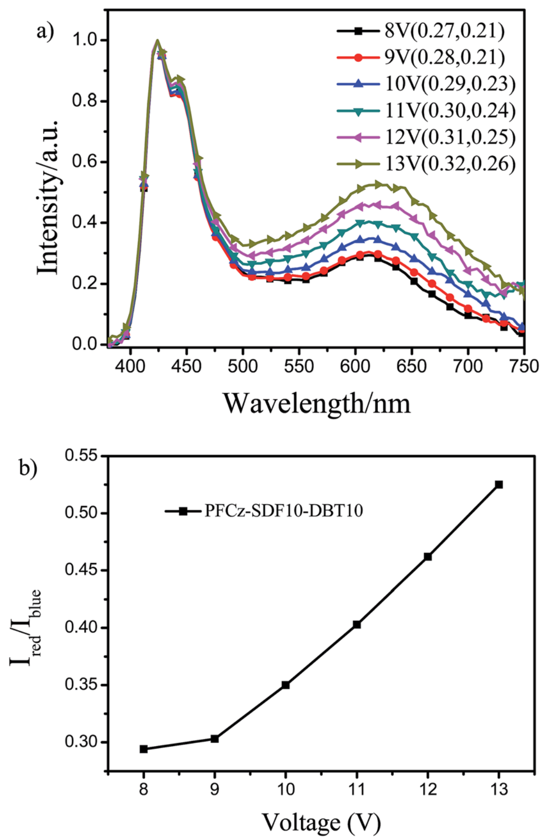

Fig. 8 Electroluminescence spectra of the copolymer **PFCzSDF10DBT10** (a), and the intensity ratio of the 610 nm of DBT emission to the 420 nm of PFCz emission of the copolymer **PFCzSDF10DBT10**, *i.e.* $R_{DBT/PFCz}$ (b).

obtained at ···V from the blue-light emitting of **PFCz** segments and the complementary orange-light emitting from **DBT** through both incomplete intra-, interchain FRET and the charge trapping processes mentioned above.

Fig. 9a shows the current density–voltage–brightness (*J*–*V*–*L*) characteristics of the devices. The devices exhibit moderate low turn-on voltage of 5.1–5.5 V (Table 4), which can be attributed to the small energy barrier between PEDOT:PSS and EML. The maximum luminance (~7400 cd m^{-2}) and maximum current efficiency (~4.2 cd A^{-1}) of the devices are quite analogous as a result of the homologous molecular structure of the copolymers. As can be seen from Fig. 9b, the efficiencies decrease quite slowly with increasing current density, suggesting that these hyperbranched copolymers and their devices have good stabilities. Further investigations on the optimization of the device performance are ongoing in our laboratory.

Conclusions

In conclusion, a series of hyperbranched 3,6-carbazole-*alt*-2,7-fluorene copolymers with **SDF** as the core were prepared by Suzuki polycondensation. The hyperbranched structures suppress the interchain interactions efficiently, and help to form amorphous spin-coating films. The emission bands of the copolymers showed no obvious bathochromic shifts in solid films with respect to those in dilute solution. The FRET efficiency from fluorene-*alt*-carbazole segments to **DBT** unit is remained in the hyperbranched systems. With the introduction of carbazole moiety into the backbone, the hyperbranched copolymers show great thermal stability with T_ds ranging from 400 to 447 °C and T_gs ranging from 178 to 186 °C, respectively. The HOMO energy levels of the copolymers were close to the work function of PEDOT:PSS because of the carbazole segment, which facilitates hole injection from PEDOT:PSS to EML in the PLEDs. Thus, the hyperbranched copolymers exhibit good EL properties with a low turn-on voltage of about 5 V, the maximum luminance of 7409.5 cd m^{-2} (at 13.5 V) and maximum current efficiency of 4.38 cd A^{-1}. **PFCzSDF10DBT8** and **PFCzSDF10DBT10** devices realized white light-emitting with CIE coordinates of (0.28, 0.31) and (0.32, 0.26),

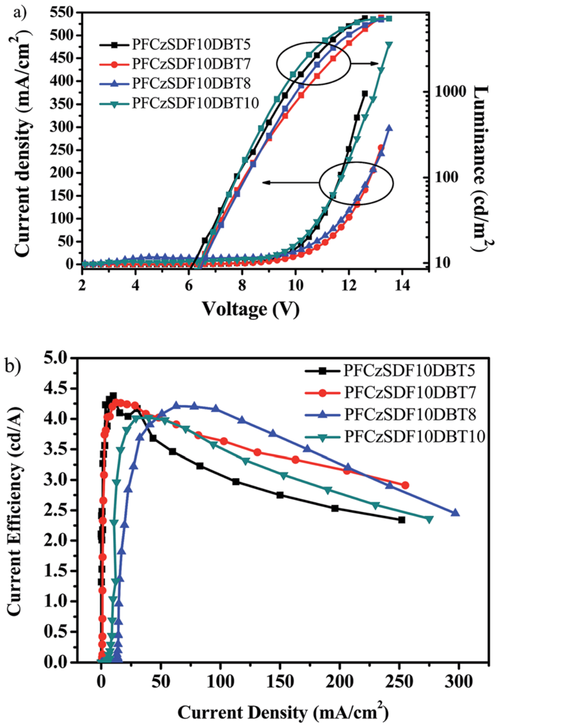

Fig. 9 Current–voltage (left) and luminance–voltage (right) curves of copolymer PLEDs (a), and current efficiency–current density characteristics of copolymer PLEDs (b).

respectively. The results indicate that the hyperbranched copolymers using **SDF** as the core and fluorene-*alt*-carbazole as the branches could be promising candidates as white-emitting materials with high efficiency.

Conflict of interest

The authors declare no competing financial interest.

Acknowledgements

The authors are grateful to the "Program for New Century Excellent Talents (NCET) in University" (NCET-13-0927), the International Science & Technology Cooperation Program of China (2012DFR50460), the National Natural Science Foundation of China (21071108, 21101111, 61274056, 61205179, 61307030, 61307029), the Qualified Personnel Foundation of Taiyuan University of Technology (QPFT) (no: tyutrc-201255a), and the Shanxi Provincial Key Innovative Research Team in Science and Technology (2012041011).

References and Notes

1 T. Guo, L. Yu, B. Zhao, Y. Li, Y. Tao, W. Yang, Q. Hou, H. Wu and Y. Cao, *Macromol. Chem. Phys.*, 2012, **213**, 820–828.
2 F. Liu, J.-Q. Liu, R.-R. Liu, X.-Y. Hou, L.-H. Xie, H.-B. Wu, C. Tang, W. Wei, Y. Cao and W. Huang, *J. Polym. Sci., Part A: Polym. Chem.*, 2009, **47**, 6451–6462.
3 W. Wu, S. Ye, L. Huang, L. Xiao, Y. Fu, Q. Huang, G. Yu, Y. Liu, J. Qin, Q. Li and Z. Li, *J. Mater. Chem.*, 2012, **22**, 6374–6382.
4 A. Pfaff and A. H. E. Müller, *Macromolecules*, 2011, **44**, 1266–1272.
5 S. H. Hwang, C. D. Shreiner, C. N. Moorefield and G. R. Newkome, *New J. Chem.*, 2007, **31**, 1192–1217.
6 C. He, L. W. Li, W. D. He, W. X. Jiang and C. Wu, *Macromolecules*, 2011, **44**, 6233–6236.
7 D. Konkolewicz, C. K. Poon, A. Gray-Weale and S. Perrier, *Chem. Commun.*, 2011, **47**, 239–241.
8 N. K. Geitner, B. Wang, R. E. Andorfer, D. A. Ladner, P. C. Ke and F. Ding, *Environ. Sci. Technol.*, 2014, **48**, 12868–12875.
9 Y. T. Tsai, C. T. Lai, R. H. Chien, J. L. Hong and A. C. Yeh, *J. Polym. Sci., Part A: Polym. Chem.*, 2012, **50**, 237–249.
10 T. Guo, R. Guan, J. Zou, J. Liu, L. Ying, W. Yang, H. Wu and Y. Cao, *Polym. Chem.*, 2011, **2**, 2193–2203.
11 R. Guan, Y. Xu, L. Ying, W. Yang, H. Wu, Q. Chen and Y. Cao, *J. Mater. Chem.*, 2009, **19**, 531–537.
12 J. Liu, L. Yu, C. Zhong, R. He, W. Yang, H. Wu and Y. Cao, *RSC Adv.*, 2012, **2**, 689–696.
13 R. Wang, W.-Z. Wang, G.-Z. Yang, T. Liu, J. Yu and Y. Jiang, *J. Polym. Sci., Part A: Polym. Chem.*, 2008, **46**, 790–802.
14 L. Y. Biqing Bao, X. Zhan and L. Wang, *Polym. Chem.*, 2010, **48**, 3431–3439.
15 L. R. Tsai and Y. Chen, *J. Polym. Sci., Part A: Polym. Chem.*, 2007, **45**, 4465–4476.
16 L. R. Tsai and Y. Chen, *Macromolecules*, 2008, **41**, 5098–5106.
17 M. C. Gather, A. Kohnen and K. Meerholz, *Adv. Mater.*, 2011, **23**, 233–248.
18 J. Liu, Y. Cheng, Z. Xie, Y. Geng, L. Wang, X. Jing and F. Wang, *Adv. Mater.*, 2008, **20**, 1357–1362.
19 L. Ying, C. L. Ho, H. Wu, Y. Cao and W. Y. Wong, *Adv. Mater.*, 2014, **26**, 2459–2473.
20 X. H. Zhu, J. Peng, Y. Cao and J. Roncali, *Chem. Soc. Rev.*, 2011, **40**, 3509–3524.
21 B. Zhang, G. Tan, C. S. Lam, B. Yao, C. L. Ho, L. Liu, Z. Xie, W. Y. Wong, J. Ding and L. Wang, *Adv. Mater.*, 2012, **24**, 1873–1877.
22 Y. Xu, H. Wang, F. Wei, J. Hou, H. Zhou and B. Xu, *Sci. China, Ser. E: Technol. Sci.*, 2009, **52**, 2190–2194.
23 H. Wang, Y. Xu, T. Tsuboi, H. Xu, Y. Wu, Z. Zhang, Y. Miao, Y. Hao, X. Liu, B. Xu and W. Huang, *Org. Electron.*, 2013, **14**, 827–838.
24 Z. Ma, S. Lu, Q.-L. Fan, C.-Y. Qing, Y.-Y. Wang, P. Wang and W. Huang, *Polymer*, 2006, **47**, 7382–7390.
25 G. Zeng, W. L. Yu, S. J. Chua and W. Huang, *Macromolecules*, 2002, **35**, 6907–6914.
26 Y. H. G. D. Katsis, J. J. Ou, S. W. Culligan, A. Trajkovska, S. H. Chen and L. J. Rothberg, *Chem. Mater.*, 2002, **14**, 1332–1339.
27 Y. Li, J. Ding, M. Day, Y. Tao, J. Lu and M. D'iorio, *Chem. Mater.*, 2004, **16**, 2165–2173.
28 J. F. Morin, M. Leclerc, D. Adès and A. Siove, *Macromol. Rapid Commun.*, 2005, **26**, 761–778.
29 J. Peng, W. L. Yu, W. Huang and J. Heeger Alan, *Adv. Mater.*, 2000, **12**, 828.

30 J. Salbeck, F. Weissörtel and J. Bauer, *Macromol. Symp.*, 1998, **125**, 121–132.
31 C. Liu, Q. Fu, Y. Zou, C. Yang, D. Ma and J. Qin, *Chem. Mater.*, 2014, **26**, 3074–3083.
32 S. Yu, H. Lin, Z. Zhao, Z. Wang and P. Lu, *Tetrahedron Lett.*, 2007, **48**, 9112–9115.
33 O. P. Y. Moll, T. Le Borgne, P. Thuéry and M. Ephritikhine, *Tetrahedron Lett.*, 2001, **42**, 3855–3856.
34 W. Shin, M. Y. Jo, D. S. You, Y. S. Jeong, D. Y. Yoon, J.-W. Kang, J. H. Cho, G. D. Lee, S.-S. Hong and J. H. Kim, *Synth. Met.*, 2012, **162**, 768–774.
35 Z. Wang, P. Lu, S. Xue, C. Gu, Y. Lv, Q. Zhu, H. Wang and Y. Ma, *Dyes Pigm.*, 2011, **91**, 356–363.
36 B. Liu, A. Najari, C. Pan, M. Leclerc, D. Xiao and Y. Zou, *Macromol. Rapid Commun.*, 2010, **31**, 391–398.
37 J. Kim, S. H. Kim, J. Kim, I. Kim, Y. Jin, J. H. Kim, H. Y. Woo, K. Lee and H. Suh, *Macromol. Res.*, 2011, **19**, 589–598.
38 H. Wang, J. T. Ryu and Y. Kwon, *J. Appl. Polym. Sci.*, 2011, **119**, 377–386.
39 T. Sudyoadsuk, P. Moonsin, N. Prachumrak, S. Namuangruk, S. Jungsuttiwong, T. Keawin and V. Promarak, *Polym. Chem.*, 2014, **5**, 3982–3993.
40 For the fluorene-based hyperbranched copolymer with SDF branch point, the absorption peak was at about 384 nm, and the emission peaks were at 420, 442, and a shoulder peak at 468 nm. This is our another work, and it will be published elsewhere.
41 J. Yang, C. Y. Jiang, Y. Zhang, R. Q. Yang, W. Yang, Q. Hou and Y. Cao, *Macromolecules*, 2004, **37**, 1211–1218.
42 Z. Wang, P. Lu, S. Xue, C. Gu, Y. Lv, Q. Zhu, H. Wang and Y. Ma, *Dyes Pigm.*, 2011, **91**, 356–363.
43 M. Zhu, Y. Li, J. Miao, B. Jiang, C. Yang, H. Wu, J. Qin and Y. Cao, *Org. Electron.*, 2014, **15**, 1598–1606.